European Journal of Medicinal Chemistry 74 (2014) 440–450

Contents lists available at ScienceDirect

European Journal of Medicinal Chemistry

journal homepage: http://www.elsevier.com/locate/ejmech

Original article

Structural optimization of indole based compounds for highly promising anti-cancer activities: Structure activity relationship studies and identification of lead molecules

Shaveta, Palwinder Singh*

UGC Sponsored Centre for Advanced Studies, Department of Chemistry, Guru Nanak Dev University, Amritsar 143005, Punjab, India

ARTICLE INFO

Article history:
Received 30 October 2013
Received in revised form
11 December 2013
Accepted 27 December 2013
Available online 8 January 2014

Keywords:
Indole
Pyrazole
Anti-cancer activity
Dihydrofolate reductase
Interactions

ABSTRACT

Based on the anti-cancer data of previous compounds, 27 more compounds were synthesized and subjected to anti-cancer screening. Compounds were tested over 60 human tumor cell lines of different types of cancer. As per the data available, some compounds exhibited appreciable anti-cancer properties over certain cell lines with their GI_{50} in nM range. With the help of UV–vis spectral studies, enzyme immunoassay and molecular modeling studies, dihydrofolate reductase was found to be the probable cellular target of the compounds under present investigation.

1. Introduction

As per the latest information available, it is estimated that if the spread of cancer continues at its present rate, it may cause over 13.1 million deaths in 2030 worldwide [1]. Irrespective of the un-tired efforts and screening of myriads of compounds for anti-cancer activities [2–4], the uncertainty about the cause of origin of cancer, limitations in its detection at early stage, its direct connection with process of cell division, metastatic nature of cancer cells and lack of drug penetration to cancer tissue are some of the features of this disease which prove as hurdles in the successful treatment of cancer [5,6]. Amongst the various approaches to treatment of cancer, chemotherapy finds a wide use during both pre-operative and post-operative conditions [7,8]. The main focus of chemotherapeutic agents is to block/slow down propagation of cancer cells for which enzymes associated with cell division are the primary targets. Ribonucleotide reductase (RNR), thymidylate synthase (TS), thymidylate phosphorylase (TP), dihydrofolate reductase (DHFR) are primarily concerned with generation of raw material for cell division [9,10] and hence they were made the targets during the design and development of anti-cancer agents. As a result some highly efficacious drugs like 5-fluorouracil [11], methotrexate [12], pemetrexed [13] etc appeared in the market with some hope for the cancer patients. In continuation to earlier reports for development of anti-cancer agents [14–17], particularly indole based compounds [14,15], here we report another set of compounds with appreciable anti-cancer activity over certain human tumor cell lines.

2. Results and discussion

2.1. Chemistry

A simple synthetic methodology was undertaken to synthesize conjugates of indole, pyrazole and barbituric acid. Compounds **2a** and **2b** were synthesized by condensation of **1a** and **1b** (1 mmol) with 1-(3-chlorophenyl)-3-methyl-2-pyrazolin-5-one (1.2 mmol) under microwave irradiation. Similarly, compounds **4a**, **b** and **5a**, **b** were prepared by irradiating the mixture of **1a**, **b** with barbituric acid and **1a**, **b** with oxindole (1,3-dihydroindol-2-one), respectively under microwaves. Compound **3a** and **b** were procured from reaction of **1a** and **b** with indolinone (1-[2,6-dichlorophenyl]-1,3-dihydroindol-2-one) in ethanol-water (1:2) in presence of NaOH (Scheme 1).

It was also planned to introduce a substituent at N-1 position of indole in compounds **2**–**5**, for which indoles **1a** and **b** were first

* Corresponding author. Tel.: +91 183 2258802 09x3495; fax: +91 183 2258819.
E-mail address: palwinder_singh_2000@yahoo.com (P. Singh).

0223-5234/$ – see front matter © 2014 Elsevier Masson SAS. All rights reserved.
http://dx.doi.org/10.1016/j.ejmech.2013.12.047

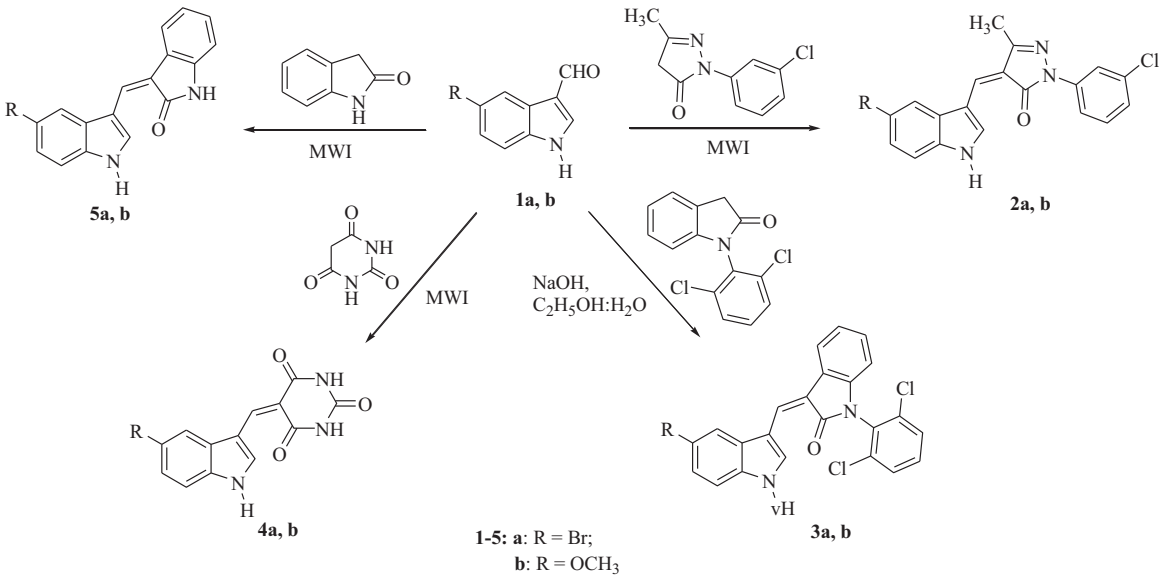

Scheme 1. Synthesis of compounds **2**–**5**.

alkylated/acylated in presence of NaH and thereby compounds **6**–**10** were prepared (Scheme 2).

Treatment of compound **6**–**9** with 1-(3-chlorophenyl)-3-methyl-2-pyrazolin-5-one/indolinone/barbituric acid/oxindole under microwave irradiation provided compounds **11**–**21** (Scheme 3).

Similarly, reactions of compound **10** with 1-(3-chlorophenyl)-3-methyl-2-pyrazolin-5-one/indolinone/barbituric acid/oxindole resulted into the formation of compounds **22**–**25** (Scheme 4).

Since trifluoromethyl group is an active component of a number of drugs, compounds **26**–**28** were prepared through condensation of 2-trifluoromethylbenzaldehyde with oxindole, indolinone and 1-(3-chlorophenyl)-3-methyl-2-pyrazolin-5-one, respectively. Further treatment of compound **26** with *p*-chlorobenzoyl chloride and 2-fluorobenzyl bromide in presence of NaH provided compounds **29** and **30** (Scheme 5). Therefore, through a very convenient synthetic protocol, a library of compounds was procured in almost quantitative yield.

2.2. Anti-cancer activity

In vitro tumor growth inhibitory activities of compounds **3a**, **3b**, **4a**, **4b**, **11**, **12**, **15**, **16**, **18**, **19**, **21**, **23**, **24**, **25**, **27**, **28** and **29** were investigated on 60 cell line panel of human cancer cells at National Cancer Institute (NCI), Bethesda, MD, USA. The compounds were found to be selective for different cell lines and anti-cancer data of compounds with significant activity over certain cancer cell lines is given in Table 1. Compound **3b** showed specificity for various cell lines of non-small cell lung cancer, colon cancer and prostate cancer. Compound **11** exhibited high selectivity for MDA-MB-468 cell line of breast cancer with GI_{50} 120 nM. Compound **12** was identified as the most potent amongst those screened here. It exhibited excellent specificity for various cell lines of leukemia along with non-small cell lung cancer, colon cancer, melanoma, prostate cancer and renal cancer. Remarkably, GI_{50} of compound **12** for NCI-H522 cell line of non-small cell lung cancer was 1 nM. Interestingly, presence of Br in compound **12** considerably increased its anti-cancer activity in comparison to its analog **31** (Chart 1), reported earlier [15]. Compounds **16**, **18**, **19** and **25** showed growth inhibition over certain cell lines with GI_{50} in μM (Table 1). Compounds **23** and **27** were more specific for various cell lines of leukemia. LC_{50} (50% lethal conc of compound) of these compounds was >100 μM indicating their appreciable selectivity indices. Therefore, results of anti-cancer screening experiments clearly indicate the potency of these compounds for controlling cancer growth over certain cell lines.

Looking at the structure activity relationship of these compounds, it is quite evident that a small variation in the structure of the compound made a dramatic change in its biological activity. Compounds **3b** and **23** with OCH_3 substituent at C-5 of indole showed better anti-cancer activity than their analogs **3a** and **15** carrying Br at C-5 of indole. 5-Unsubstituted indole-pyrazole adduct (**32**, Chart 1) [15] did not show anticancer activity but with introduction of Br at C-5 position of indole, the resulting compound **2a** exhibited appreciable anticancer activity [16]. Moreover, far better GI_{50} of compound **12** in comparison to that of compound **2a** indicates the role of substituent at N-1 of indole in increasing the anti-cancer potency of compound **12**. The substituent specificity was observed by replacing *p*-chlorobenzoyl group of compound **12** with 2,6-dichlorobenzoyl in compound **14** which made compound **14** inactive towards anti-cancer activity. Similarly, comparison of compounds **11** and **22** indicates that presence of Br in compound **11** made it selective towards MDA-MB-468 cell line of breast cancer. It means instead of a single substituent, the biological activity of the compound is decided by the combination of all the

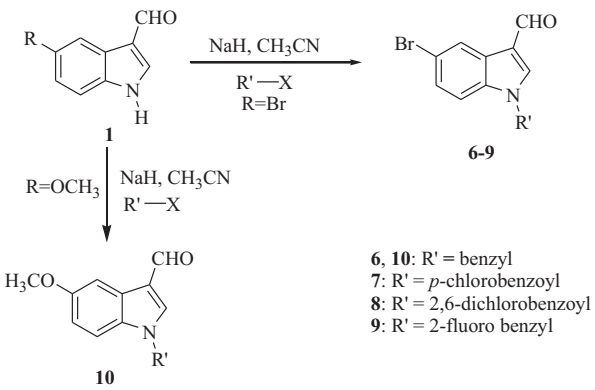

Scheme 2. Synthesis of compounds **6**–**10**.

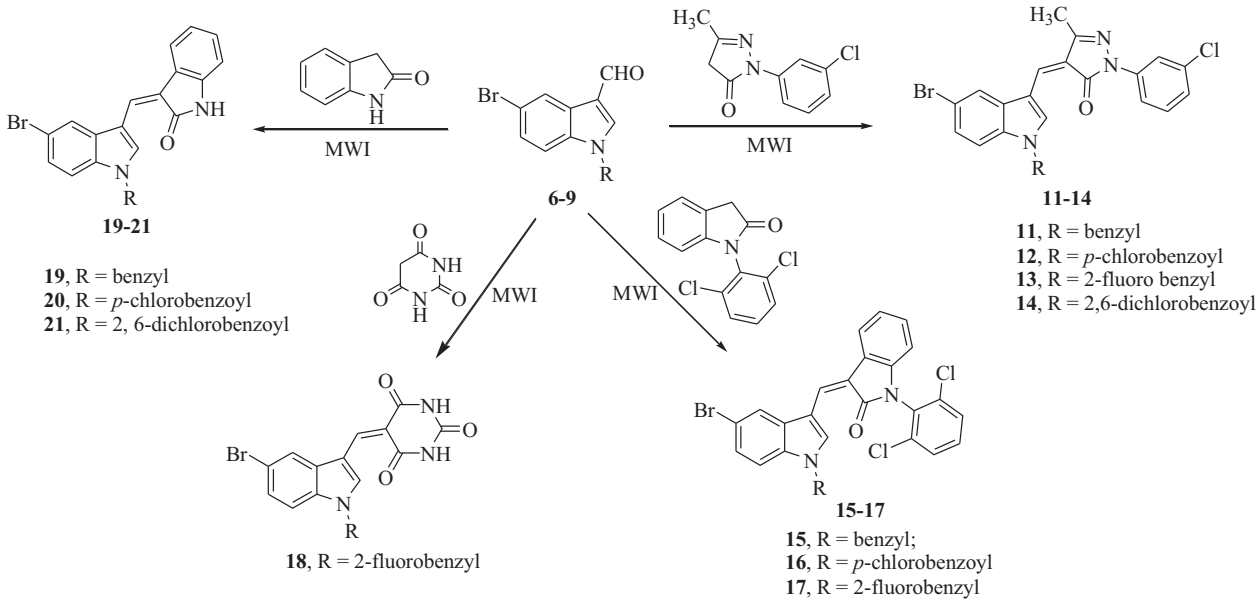

Scheme 3. Synthesis of compounds **11**–**21**.

fragments of the molecule. Trifluorotolyl substituent showed its effect for anti-cancer activity only in combination with indolinone moiety (compound **27**). Also, by comparing the anti-cancer activity of compounds **23** and **25**, it was observed that presence of 2,6-dichlorophenyl moiety in compound **23** made it more potent against various cell lines of non-small cell lung cancer and colon cancer. In comparison to the anti-cancer activity of one of our previous compounds (**33**, Chart 1) [14], presence of OCH_3 group in compound **24** made it inactive for cancer growth inhibition.

Appreciable anti-cancer activity of compounds **12** and **16** amongst their respective groups (**11**–**14** and **15**–**17**) points towards the suitability of indole–pyrazole and indole–indolinone in combination with *p*-chlorobenzoyl group for anti-cancer activity. Therefore, considerable success was attained in optimizing the structure of compound **12** and getting a promising lead molecule for anti-cancer drug.

2.3. Mechanistic investigations of mode of action of test compounds

Based on the anti-cancer activities of the compounds, it was desirable to investigate their probable cellular target and hence mode of action. Interactions of the compounds with RNR, TS, TP and DHFR, the enzymes involved in the process of propagation of cancer, were investigated with the help of UV–vis spectral studies, enzyme immunoassay and molecular modeling though the other cellular target/s of these compounds cannot be ruled out. It was envisaged that these studies may help in further refinement of the compounds for increasing their drug efficacy and also to check if the compounds exhibit promiscuity or not.

2.3.1. UV–visible spectral studies

UV–visible spectral studies were performed to analyze the interaction of the compounds with enzymes. The compounds were

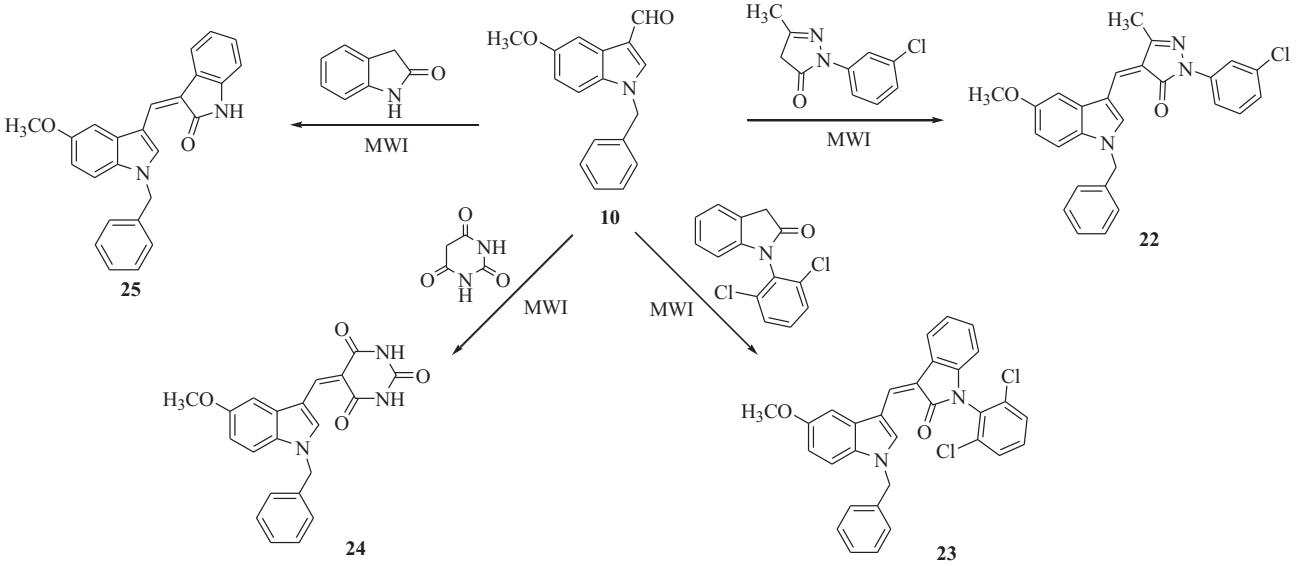

Scheme 4. Synthesis of compounds **22**–**25**.

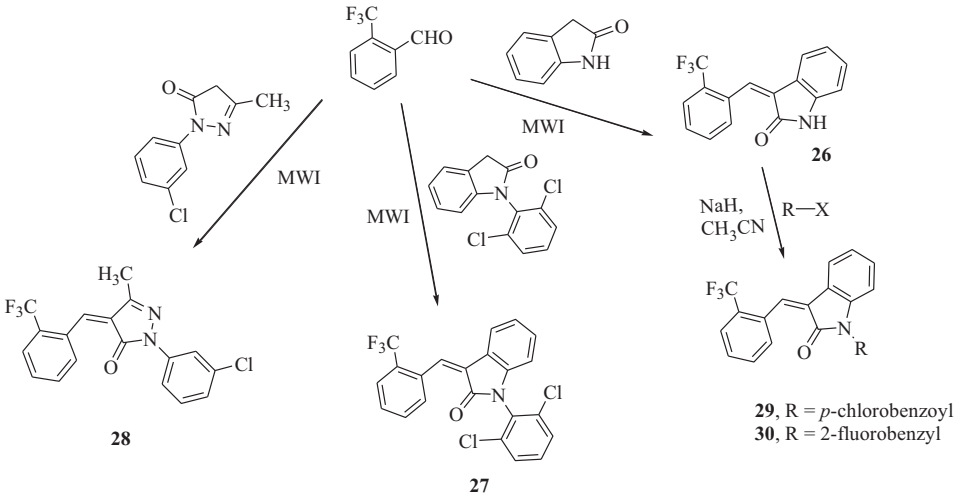

Scheme 5. Synthesis of compounds **26**–**30**.

evaluated at a concentration varying from 1 μM to 5 μM by preparing the stock solutions in DMSO. The enzyme (0.1 units) was used as supplied. For studying the enzyme–compound interactions, 50 μL of the enzyme was used and diluted to 1000 μL. The compound solution was added to the enzyme solution by varying the concentration from 1 μM to 5 μM. To our surprise, addition of compounds to solution of RNR, TS and TP did not make change in the UV spectra of these enzymes. Checking in another way, addition of enzyme RNR, TS and TP to the solution of compounds also did not change UV–vis spectrum of the compound. However, appreciable change in the UV–vis spectrum of compound **12** was observed when it was added to solution of DHFR. Compound **12** (5 μM solution in DMSO) showed two λ_{max} at 260 nm and 397 nm in its UV–vis spectrum (Fig. S45). In presence of DHFR (50 μL), the peak at 260 nm showed a bathochromic shift to 268 nm along with hyperchromic shift at both the absorption maxima (Fig. S45). Similar observations were noticed with compounds **3b** and **27**.

Therefore, a simple assay indicates the non-promiscuous nature of the compounds amongst the four enzymatic targets (RNS, TS, TP and DHFR) and hence they may not be the frequent hitters. Rather the active compounds seem to be targeting a particular enzyme.

2.3.2. Enzyme inhibition assay

Further, to confirm the interaction of compounds with DHFR and probably the inhibition in enzymatic activity of DHFR in presence of compounds, DHFR enzyme immunoassay was

Table 1
GI_{50} (50% growth inhibitory conc) of compounds **3b**, **11**, **12**, **16**, **18**, **19**, **23**, **25** and **27** over various cancer cell lines.

Panel/cell line	GI_{50} (μM)								
	3b	**11**	**12**	**16**	**18**	**19**	**23**	**25**	**27**
Leukemia									
CCRF-CEM	22	50	0.03	0.11	>100	>100	0.13	>100	58
HL-60(TB)	18	57	1.5	>100	>100	82	>100	>100	1.1
K-562	25	48	1.5	60	>100	75	0.10	>100	1.4
MOLT-4	25	35	0.04	62	>100	>100	1.5	>100	0.10
RPMI-8226	30	>100	0.01	>100	>100	>100	0.14	>100	1.4
SR	>100	>100	0.02	>100	>100	>100	1.4	>100	2.0
Non-small cell lung cancer									
HOP-62	>100	>100	48	>100	>100	>100	>100	1.41	>100
HOP-92	1.4	>100	45	0.20	>100	>100	>100	1.6	1.5
NCI-H322M	>100	>100	1.4	>100	>100	>100	>100	>100	>100
NCI-H460	1.6	>100	>100	>100	>100	0.23	>100	>100	1.6
NCI-H522	1.10	>100	0.001	>100	>100	>100	>100	>100	>100
Colon cancer									
HCT-116	1.80	>100	64	>100	1.5	1.5	1.22	>100	1.4
HCT-15	1.42	>100	0.02	3.0	>100	>100	>100	>100	2.5
HT29	3.0	>100	0.01	>100	>100	>100	>100	>100	>100
KM12	3.4	>100	1.5	>100	>100	>100	>100	>100	>100
Melanoma									
MALME-3M	>100	>100	0.02	0.12	>100	>100	>100	>100	>100
Renal cancer									
CAKI-1	>100	>100	0.12	>100	>100	>100	>100	>100	>100
UO-31	>100	>100	>100	1.4	>100	>100	>100	2.4	>100
Prostate cancer									
PC-3	1.53	>100	0.01	>100	1.2	>100	>100	>100	2.10
Breast cancer									
[MDA-MB-231/ATCC]	>100	>100	>100	0.12	1.22	>100	>100	>100	>100
T-47D	>100	>100	>100	>100	>100	1.34	>100	>100	1.42
[MDA-MB-468]	>100	0.12	42	>100	>100	>100	0.01	>100	>100
MCF7	>100	>100	0.02	>100	>100	>100	>100	>100	>100

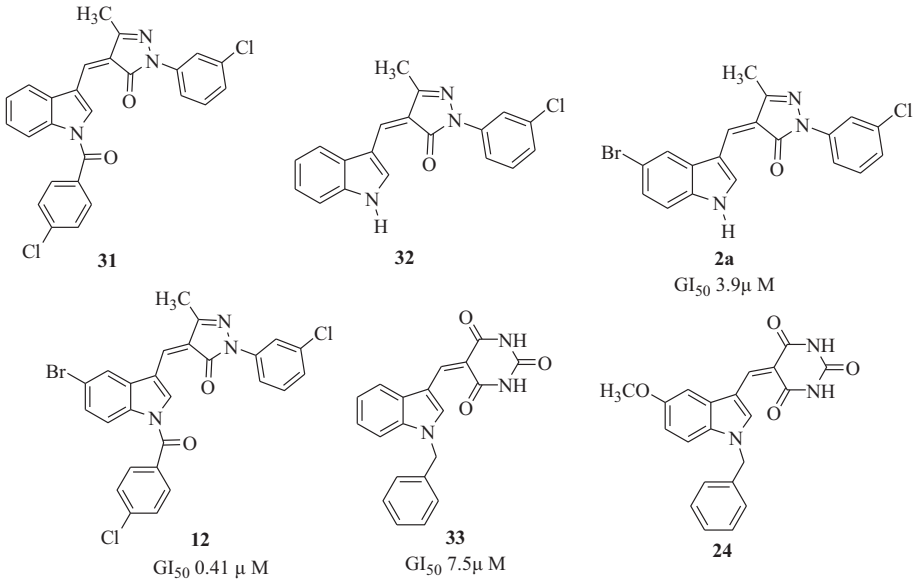

Chart 1. Structural comparison of compounds **12** and **24** with previously reported compounds **2a** and **31**–**33**. GI_{50} is the average over all the cancer cell lines. GI_{50} for compounds **31** and **32** were not available.

performed using dihydrofolate reductase inhibition assay kit [18]. Some of the compounds showed excellent inhibitory activity with IC_{50} ranging from μM to nM (Table 2) and comparable to the standard drug methotrexate. Compounds **3b** and **12** showed IC_{80} 0.10 μM and 0.28 μM, respectively for DHFR while IC_{50} of compounds **25** and **27** was calculated as 54 nM and 68 nM, respectively. Therefore, it seems that the compounds under present investigation probably target DHFR for exhibiting anti-cancer activities. However, compounds **19**, **23** and **24** did not show inhibition of DHFR enzymatic activity.

2.3.3. Molecular docking studies

In order to have an insight into the molecular interactions of the compounds with DHFR, their docking in the active site of the enzyme was performed. The crystal coordinates of DHFR in complexation with an anti-cancer agent were taken from protein data bank (www.rcsb.org) (PDB ID 3GHW) [19]. Compounds **12**, **3b** and **27** were docked in the active site of DHFR. Compound **12** sits in the active site of the enzyme interacting through H-bonding between pyrazolic N and Gln35 residue of α-helical part of the enzyme (Fig. 1, Fig. S47). The indole part of the compound aligns in parallel with one β-sheet (yellow in color) while its *p*-chlorobenzoyl fragment overlaps with another β-sheet (blue in color) indicating the favorable hydrophobic interactions of the indole moiety and polar interactions from the *p*-chlorobenzoyl group.

CPK model of the DHFR active site also clearly shows the compatibility of compound **12** in the active site of the enzyme (Fig. 2). Similar mode of interaction of compound **3b** (Figs. 3 and 4, Fig. S46) and **27** (Figs. S48 and S49) was observed when docked in the active site of DHFR. Therefore, the crystal coordinates of the enzyme in association with compound **12**, **3b** and **27** support the experimental results of interactions and enzyme inhibitory activities of these compounds.

3. Conclusions

A number of compounds, significantly important for structure activity relationship studies, were synthesized using a simple synthetic methodology. Anti-cancer screening of these compounds identified compound **12** with considerable specificity for NCI-H522 cell line of non-small cell lung cancer where it exhibited GI_{50} 1 nM. Compound **12** along with some other compounds also showed appreciable inhibition of tumor growth over different cell lines of leukemia, non-small cell lung cancer, colon cancer and prostate cancer. Over all, modification of previously reported compounds led to the development of highly potent compounds against certain types of cancer. Mechanistic investigations of mode of action of these compounds point towards the possibility of DHFR as their cellular target. Therefore, stepwise modification of the compounds led to considerable success in the search of some highly promising leads for anti-cancer drugs.

4. Experimental data

4.1General remarks

Melting points were determined in capillaries and are uncorrected. IR spectra were recorded on PerkinElmer Fourier Transform Infrared spectrometer. ^1H and ^{13}C NMR spectra were recorded on JEOL 300 MHz and 75 MHz NMR spectrometer, respectively using $CDCl_3$ and/or DMSO-d_6 as solvent. Chemical shifts are given in ppm with TMS as an internal reference. *J* values are given in Hertz. Signals are abbreviated as singlet, s; doublet, d; double-doublet, dd;

Table 2
IC_{50} (50% inhibitory concentration) for compounds **3b**, **11**, **12**, **16**, **18**, **19**, **23**, **24**, **25** and **27** for dihydrofolate reductase (DHFR).

Compound	IC_{50} (μM)
3b	0.10[a]
11	1.25
12	0.28[a]
16	0.69
18	0.30
19	–
23	–
24	–
25	53.9[b]
27	67.7[b]
Methotrexate	1.39

[a] Corresponds to IC_{80}.
[b] IC_{50} in nM.

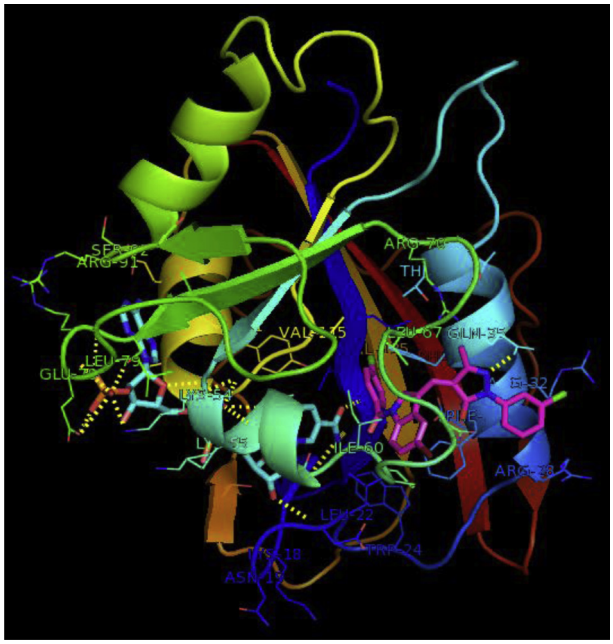

Fig. 1. Crystal coordinates of DHFR in complexation with compound **12** (pink) (generated in pymol). H-Bond between pyrazole N of compound **12** and Gln35 is visible. (For interpretation of the references to color in this figure legend, the reader is referred to the web version of this article.)

triplet, t; multiplet, m. In ^{13}C NMR spectral data, +ve, −ve terms correspond to CH_3, CH, CH_2 signals in DEPT-135 NMR spectra. Mass spectra were recorded on Bruker MicroTOF QII mass spectrometer in +ve ESI mode with capillary voltage 4500 V except for compound **4a** and **12** (recorded in APCI mode, in solid state). Chromatography was performed with silica 100–200 mesh and reactions were monitored by thin layer chromatography (TLC) with silica plates coated with silica gel GF-254. Reactions under microwaves were performed using microwave oven (INALSA model 1MW17EG) with microwave power 700 W and operating frequency 2450 MHz. UV–visible spectral studies were performed on Biotek PowerwaveXS spectrophotometer to analyze the interaction of the compounds with enzymes.

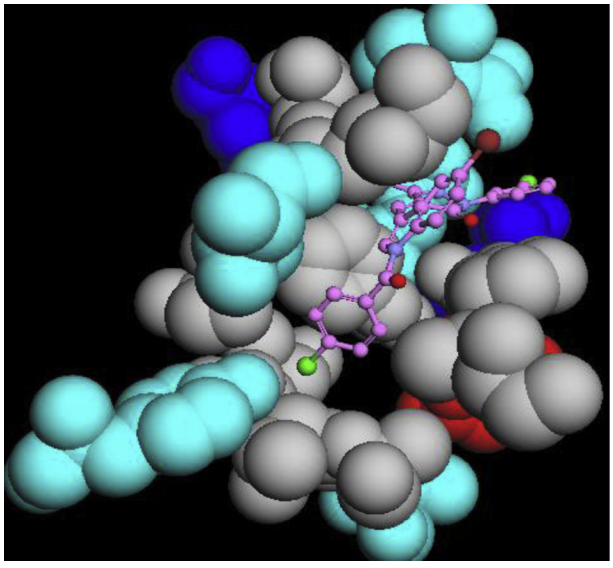

Fig. 2. CPK model of active site of DHFR with docking of compound **12**.

*4.1.1. General procedure for synthesis of compounds **2**–**5** and **11**–**28** (Procedure A)*

A finely ground mixture of 5-substituted indole-3-carboxaldehyde (1 mmol) and active methylene compound (indolinone/oxindole/barbituric acid/1-(3-chlorophenyl)-3-methyl-2-pyrazolin-5-one)/2-trifluoromethylbenzaldehyde (1.2 mmol) was irradiated in microwave oven for 1–5 min. The solid product was washed with diethyl ether and purified by column chromatography to get pure products **2**–**5** and **11**–**28** except compound **3**. Compound **3** was prepared by treatment of 5-substituted indole-3-carboxaldehyde with indolinone in ethanol-water in presence of NaOH (1.5 mmol).

*4.1.2General procedure for synthesis of compounds **6**–**10** (Procedure B)*

Sodium hydride (NaH, 1.5 mmol) was washed with hexane several times to remove all the paraffin and then suspended in acetonitrile (ACN). 5-Br/OCH_3 indole-3-carboxaldehyde (**1**, 1 mmol) was added to the suspension of NaH in ACN and kept stirred at 0 °C. Reaction progress was monitored by TLC. Reaction was complete in 30 min. The reaction mixture was extracted with ethyl acetate followed by washing of organic layer with water. The organic layer was passed through anhydrous Na_2SO_4 and concentrated to give crude products **6**–**10** which were later purified by washing with hexane.

*4.1.3. General procedure for synthesis of compounds **29** and **30***

Compound **29** and **30** were prepared by following the same procedure as (B) starting with compound **26** (1 mmol).

*4.1.4. 4-(5-Bromo-1H-indol-3-ylmethylene)-2-(3-chlorophenyl)-5-methyl-2,4-dihydropyrazol-3-one, **2a***

Pure product was obtained as an orange solid in a yield of 65%, mp 280 °C (decomposed); IR ν_{max} (KBr, cm^{-1}): 1645 (C=O), 3164 (NH); ^1H NMR (300 MHz, DMSO-d_6) δ ppm: 2.40 (s, 3H, CH_3), 7.20 (d, J = 9.0 Hz, 1H, ArH), 7.43 (t, J = 9.0 Hz, 2H, ArH), 7.53 (d, J = 8.4 Hz, 1H, ArH), 7.94 (d, J = 8.1 Hz, 1H, ArH), 8.13 (d, J = 9.0 Hz, 2H, ArH), 8.49 (s, 1H, bridged =CH), 9.70 (s, 1H, indole 2-H), 12.7 (NH, D_2O exchange); ^{13}C NMR (normal/DEPT-135) (DMSO + $CDCl_3$) δ ppm: 13.02 (+ve, CH_3), 111.779 (C), 114.507 (+ve, CH), 115.142 (C), 115.81 (+ve, CH), 117.19 (+ve, CH), 118.61 (C), 121.23 (+ve, CH), 123.22 (+ve, CH), 125.86 (+ve, CH), 129.96 (+ve, CH), 133.29 (C), 135.13 (C), 137.29 (+ve, CH), 139.02 (+ve, CH), 139.93 (C), 151.43 (C), 162.85 (C=O); HRMS (ESI) Calcd for $C_{19}H_{13}BrClON_3$: 435.9823, 437.9802. Found: m/z 435.9808, 437.9788 $([M + Na])^+$.

*4.1.5. 2-(3-Chlorophenyl)-4-(5-methoxy-1H-indol-3-ylmethylene)-5-methyl-2,4-dihydro-pyrazol-3-one, **2b***

Pure product was obtained as an orange solid in a yield of 80%, mp 239–240 °C; IR ν_{max} (KBr, cm^{-1}): 1649 (C=O), 3169 (NH); ^1H NMR (300 MHz, DMSO-d_6) δ ppm: 2.45 (s, 3H, CH_3), 3.93 (s, 3H, OCH_3), 6.92 (d, J = 8.4 Hz, 1H, ArH), 7.11 (d, J = 7.5 Hz, 1H, ArH), 7.32–7.43 (m, 2H, ArH), 7.75 (s, 1H, ArH), 7.89 (s, 1H, ArH), 7.89 (s, 1H, ArH), 8.01 (d, J = 8.1 Hz, 1H, ArH), 8.15 (s, 1H, bridged =CH), 9.82 (s, 1H, indole 2-H), 12.26 (s, 1H, NH); HRMS (ESI) Calcd for $C_{20}H_{16}ClO_2N_3$: 388.0823. Found: m/z 388.0839 $([M + Na])^+$.

*4.1.6. 3-(5-Bromo-1H-indol-3-ylmethylene)-1-(2,6-dichlorophenyl)-1,3-dihydroindol-2-one, **3a***

Pure product was obtained as a yellow solid in a yield of 77%, mp 275–277 °C; IR ν_{max} (KBr, cm^{-1}): 1676 (C=O), 3268 (NH); ^1H NMR (300 MHz, $CDCl_3$) δ ppm: 6.48 (d, J = 7.2 Hz, 1H, ArH), 7.19 (d, J = 7.2 Hz, 3H, ArH), 7.35–7.45 (m, 2H, ArH), 7.51–7.58 (m, 2H, ArH),

Fig. 3. Crystal coordinates of DHFR with compound **3b** (pink). H-Bond between 5-methoxy O of compound **3b** and Gln35 is visible. NADPH is also visible. (For interpretation of the references to color in this figure legend, the reader is referred to the web version of this article.)

7.76 (d, J = 6.0 Hz, 1H, ArH), 8.01 (s, 1H, bridged =CH), 8.07 (s, 1H, ArH), 9.31 (s, 1H, NH), 9.55 (s, 1H, indole 2-H); ^{13}C NMR ($CDCl_3$) δ ppm: 108.87, 110.52, 112.48, 113.27, 115.06, 118.50, 121.60, 122.50, 125.96, 127.65, 128.98, 130.64, 130.67, 133.30, 134.60, 135.95, 166.42 (C=O); HRMS (ESI) Calcd for $C_{23}H_{13}BrCl_2ON_2$: 504.9481, 506.9459, 508.9431. Found: m/z 504.9472, 506.9453, 508.9445 $([M + Na])^+$.

4.1.7. 1-(2,6-Dichlorophenyl)-3-(5-methoxy-1H-indol-3-ylmethylene)-1,3-dihydroindol-2-one, **3b**

Pure product was obtained as a yellow solid in a yield of 69%, mp 246–247 °C; IR ν_{max} (KBr, cm^{-1}): 1680 (C=O), 3260 (NH); ^{1}H NMR (300 MHz, $CDCl_3$) δ ppm: 3.94 (s, 3H, OCH_3), 6.45 (d, J = 8.1 Hz, 1H, ArH), 6.91 (d, J = 8.7 Hz, 1H, ArH), 7.14–7.16 (m, 2H, ArH), 7.35–7.41 (m, 3H, ArH), 7.53 (d, J = 8.1 Hz, 2H, ArH), 7.75 (d, J = 5.7 Hz, 1H, ArH), 8.05 (s, 1H, bridged =CH), 9.02 (s, 1H, NH), 9.50 (s, 1H, indole 2-H); ^{13}C NMR (DEPT-135) ($CDCl_3$) δ ppm: 56.01 (+ve, OCH_3), 100.45 (+ve, CH), 108.75 (+ve, CH), 110.14 (C), 112.59 (+ve, CH), 112.76 (+ve, CH), 115.60 (C), 118.16 (+ve, CH), 122.26 (C), 123.34 (C), 128.17 (+ve, CH), 128.95 (C), 130.50 (+ve, CH), 130.69 (C), 131.23 (+ve, CH), 133.83 (C), 136.05 (C), 136.82 (C), 138.85 (C), 155.73 (C=O); HRMS (ESI) Calcd for $C_{24}H_{16}Cl_2O_2N_2$: 435.0662, 437.0634. Found: m/z 435.0396, 437.0376 $([M + H])^+$.

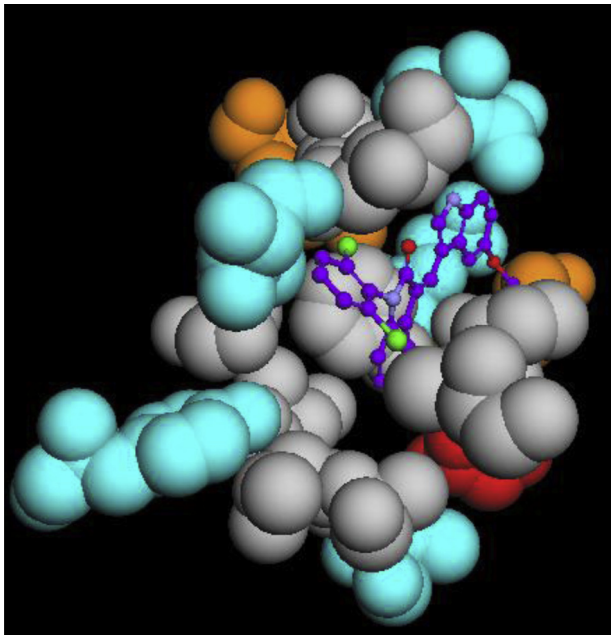

Fig. 4. CPK model of active site of DHFR with docking of compound **3b**.

4.1.8. 5-(5-Bromo-1H-indol-3-ylmethylene)-pyrimidine-2,4,6-trione, **4a**

Pure product was obtained as a yellow solid in a yield of 77%, mp >300 °C; IR ν_{max} (KBr, cm^{-1}): 1650, 1689, 1728 (C=O), 3170 (NH); ^{1}H NMR (300 MHz, DMSO-d_6) δ ppm: 7.40 (d, J = 8.4 Hz, 1H, ArH), 7.52 (d, J = 8.1 Hz, 1H, ArH), 7.98 (s, 1H, bridged =CH), 8.64 (s, 1H, ArH), 9.51 (s, 1H, indole 2-H), 11.08 (s, 1H, NH), 11.16 (s, 1H, NH), 12.77 (s, 1H, NH); ^{13}C NMR ($CDCl_3$ + DMSO-d_6) δ ppm: 101.85, 109.13, 110.78, 113.42, 114.77, 130.05, 130.97, 135.07, 140.26, 143.46, 150.28, 156.35 (C=O), 162.49 (C=O), 164.32 (C=O); HRMS (APCI) Calcd for $C_{13}H_8BrO_3N_3$: 332.9744, 334.9723. Found: m/z 332.9465, 334.9465 $([M])^+$.

4.1.9. 5-(5-Methoxy-1H-indol-3-ylmethylene) pyrimidine-2,4,6-trione, **4b**

Pure product was obtained as a yellow solid in a yield of 60%, mp >300 °C; IR ν_{max} (KBr, cm^{-1}): 1650, 1685 (C=O), 3181, 3344, 3480 (NH); ^{1}H NMR (300 MHz, DMSO-d_6) δ ppm: 3.89 (s, 3H, OCH_3), 6.90 (d, J = 8.7 Hz, 1H, ArH), 7.42 (d, J = 8.7 Hz, 1H, ArH), 8.04 (s, 1H, bridged =CH), 8.74 (s, 1H, ArH), 9.52 (s, 1H, indole 2-H), 10.95 (s, 1H, NH), 11.02 (s, 1H, NH), 12.51 (s, 1H, NH); ^{13}C NMR ($CDCl_3$ + DMSO-d_6) δ ppm: 55.23 (OCH_3), 99.71, 107.23, 111.77, 112.85, 113.50, 130.20, 130.95, 131.29, 140.08, 144.21, 150.30, 155.95 (C=O), 163.08 (C=O), 164.68 (C=O); HRMS (ESI) Calcd for $C_{14}H_{11}O_4N_3$: 308.0642, Found: m/z 308.0658 $([M + Na])^+$.

4.1.10. 3-(5-Bromo-1H-indol-3-ylmethylene)-1,3-dihydroindol-2-one, **5a**

Pure product was obtained as a pale yellow solid in a yield of 76%, mp 270 °C (decomposed); IR ν_{max} (KBr, cm^{-1}): 1678 (C=O), 3210, 3408 (NH); ^{1}H NMR (300 MHz, DMSO-d_6) δ ppm: 6.83–6.99 (m, 2H, ArH), 7.09–7.19 (m, 1H, ArH), 7.29–7.34 (m, 1H, ArH), 7.42–7.49 (m, 1H, ArH), 7.72–7.86 (m, 2H, ArH), 8.12 (s, 1H, bridged =CH), 9.47 (s, 1H, indole 2-H), 10.42 (s, 1H, NH), 12.04 (s, 1H, NH); ^{13}C NMR (DEPT-135) ($CDCl_3$ + DMSO-d_6) δ ppm: 108.77 (+ve, CH), 110.73 (C), 113.65 (+ve, CH), 120.63 (+ve, CH), 124.61 (+ve, CH), 124.93 (C), 125.38 (C), 126.13 (+ve, CH), 126.53 (+ve, CH), 128.08 (C), 129.80 (C), 134.25 (+ve, CH), 139.09 (C), 141.63 (C), 168.05 (C=O); HRMS (ESI) Calcd for $C_{17}H_{13}BrON_2$: 363.0103, 365.0084. Found: m/z 363.0131, 365.0089 $([M + Na])^+$.

4.1.11. 3-(5-Methoxy-1H-indol-3-ylmethylene)-1,3-dihydroindol-2-one, **5b**

Pure product was obtained as a yellow solid in a yield of 74%, mp 240 °C (decomposed); IR ν_{max} (KBr, cm^{-1}): 1678 (C=O), 3221, 3361 (NH); ^{1}H NMR (300 MHz, DMSO-d_6) δ ppm: 3.93 (s, 3H, OCH_3), 6.87–7.12 (m, 4H, ArH), 7.37 (d, J = 9.0 Hz, 2H, ArH), 7.68 (s, 1H, ArH), 7.94 (s, 1H, bridged =CH), 9.47 (s, 1H, indole 2-H), 10.13 (s, 1H, NH), 11.52 (s, 1H, NH); HRMS (ESI) Calcd for $C_{18}H_{14}O_2N_2$: 291.1128. Found: m/z 291.1146 $([M + H])^+$.

4.1.12. 4-(1-Benzyl-5-bromo-1H-indol-3-ylmethylene)-2-(3-chlorophenyl)-5-methyl-2,4-dihydropyrazol-3-one, ***11***

Pure product was obtained as an orange solid in a yield of 69%, mp 217–219 °C; IR ν_{max} (KBr, cm^{-1}): 1683 (C=O); ^1H NMR (300 MHz, $CDCl_3$) δ ppm: 2.35 (s, 3H, CH_3), 5.39 (s, 2H, CH_2), 7.05–7.16 (m, 4H, ArH), 7.19 (s, 1H, ArH), 7.24–7.31 (m, 4H, ArH), 7.63 (s, 1H, ArH), 7.88 (d, J = 8.1 Hz, 1H, ArH), 7.93 (s, 1H, ArH), 8.03 (s, 1H, bridged =CH), 9.87 (s, 1H, indole 2-H); ^{13}C NMR (DEPT-135) ($CDCl_3$) δ ppm: 13.15 (+ve, CH_3), 51.85 (−ve, CH_2), 111.40 (C), 112.90 (+ve, CH), 116.45 (C), 116.70 (+ve, CH), 118.85 (+ve, CH), 120.53 (C), 121.03 (+ve, CH), 124.31 (+ve, CH), 126.73 (+ve, CH), 128.38 (+ve, CH), 129.09 (+ve, CH), 129.73 (+ve, CH), 134.49 (C), 134.66 (+ve, CH), 134.94 (C), 135.38 (C), 139.91 (C), 141.48 (C), 150.78 (C), 163.31 (C=O); HRMS (ESI) Calcd for $C_{26}H_{19}BrClON_3$: 526.0292, 528.0272, Found: m/z 526.0339, 528.0326 $([M + Na])^+$.

4.1.13. 4-[5-Bromo-1-(4-chlorobenzoyl)-1H-indol-3-ylmethylene]-2-(3-chlorophenyl)-5-methyl-2,4-dihydropyrazol-3-one, ***12***

Pure product was obtained as a reddish orange solid in a yield of 79%, mp >300 °C; IR ν_{max} (KBr, cm^{-1}): 1679, 1700 (C=O); ^1H NMR (300 MHz, TFA + $CDCl_3$) δ ppm: 2.78 (s, 3H, CH_3), 7.27–7.81 (m, 10H, ArH), 8.11–8.28 (m, 2H, ArH), 8.47 (s, 1H, ArH); HRMS (APCI) Calcd for $C_{26}H_{16}N_3O_2BrCl_2$: 551.9876, 553.9855, 555.9827. Found: 551.9850, 553.9824, 555.9807 $([M + H])^+$.

4.1.14. 4-[5-Bromo-1-(2-fluorobenzyl)-1H-indol-3-ylmethylene]-2-(3-chlorophenyl)-5-methyl-2,4-dihydropyrazol-3-one, ***13***

Pure product was obtained as an orange solid in a yield of 85%, mp 238–240 °C; IR ν_{max} (KBr, cm^{-1}): 1673 (C=O); ^1H NMR (300 MHz, $CDCl_3$) δ ppm: 2.43 (s, 3H, CH_3), 5.51 (s, 2H, CH_2), 7.00–7.15 (m, 4H, ArH), 7.24–7.42 (m, 4H, ArH), 7.70 (s, 1H, ArH), 7.96 (d, J = 8.4 Hz, 1H, ArH), 8.01 (s, 1H, bridged =CH), 8.09 (s, 1H, ArH), 9.96 (s, 1H, indole 2-H); ^{13}C NMR (DEPT-135) ($CDCl_3$) δ ppm: 13.16 (+ve, CH_3), 50.62 (−ve, CH_2), 111.57 (C), 112.63 (+ve, CH), 116.60 (C), 116.95 (+ve, CH), 119.09 (+ve, CH), 120.60 (C), 121.09 (+ve, CH), 122.52 (C), 124.53 (C), 124.83 (+ve, CH), 126.94 (+ve, CH), 128.86 (C), 129.79 (+ve, CH), 130.36 (C), 130.90 (C), 134.51 (C), 134.94 (+ve, CH), 135.29 (C), 138.05 (C), 139.76 (C), 141.55 (+ve, CH), 150.92 (+ve, CH), 163.26 (C=O); HRMS (ESI) Calcd for $C_{26}H_{18}BrClFON_3$: 544.0198, 546.0178, Found: m/z 543.9566, 545.9546 $([M + Na])^+$.

4.1.15. 4-{5-Bromo-1-[1-(2,6-dichlorophenyl)-vinyl]-1H-indol-3-ylmethylene}-2-(3-chloro-phenyl)-5-methyl-2,4-dihydropyrazol-3-one, ***14***

Pure product was obtained as an orange solid in a yield of 73%, mp 265 °C; IR ν_{max} (KBr, cm^{-1}): 1687, 1714 (C=O); ^1H NMR (300 MHz, $CDCl_3$) δ ppm: 2.39 (s, 3H, CH_3), 7.12 (d, J = 7.5 Hz, 1H, ArH), 7.30 (d, J = 8.1 Hz, 1H, ArH), 7.52–7.56 (m, 4H, ArH), 7.66 (d, J = 8.4 Hz, 1H, ArH), 7.78 (d, J = 7.5 Hz, 1H, ArH), 7.96 (s, 2H, bridged =CH, ArH), 8.59 (d, J = 8.4 Hz, 1H, ArH), 9.53 (s, 1H, indole 2-H); HRMS (ESI) Calcd for $C_{26}H_{15}BrCl_3O_2N_3$: 585.9486, 587.9465, 589.9437. Found: m/z 585.9502, 587.9491, 589.9482 $([M + H])^+$.

4.1.16. 3-(1-Benzyl-5-bromo-1H-indol-3-ylmethylene)-1-(2,6-dichlorophenyl)-1,3-dihydro-indol-2-one, ***15***

Pure product was obtained as a yellow solid in a yield of 73%, mp 140 °C; IR ν_{max} (KBr, cm^{-1}): 1701 (C=O); ^1H NMR (300 MHz, $CDCl_3$) δ ppm: 5.37 (s, 1H, CH_2), 6.47 (d, J = 7.2 Hz, 1H, ArH), 7.12–7.18 (m, 6H, ArH), 7.28–7.41 (m, 4H, ArH), 7.55 (d, J = 7.8 Hz, 2H, ArH), 7.76 (d, J = 6.3 Hz, 1H, ArH), 7.99 (s, 1H, ArH), 8.08 (s, 1H, bridged =CH), 9.58 (s, 1H, indole 2-H); ^{13}C NMR (DEPT-135) ($CDCl_3$) δ ppm: 51.44 (−ve, CH_2), 108.79 (C), 110.91 (C), 112.41 (+ve, CH), 115.23 (C), 118.38 (+ve, CH), 118.66 (C), 121.01 (+ve, CH), 122.36 (+ve, CH), 125.88 (+ve, CH), 126.62 (+ve, CH), 126.93 (C), 127.24 (+ve, CH), 128.03 (+ve, CH), 128.94 (+ve, CH), 129.10 (C), 130.52 (+ve, CH), 134.93 (C), 135.75 (C), 135.96 (C), 138.38 (C), 154.73 (C), 165.20 (C=O); HRMS (ESI) Calcd for $C_{30}H_{19}BrCl_2ON_2$: 573.0131, 575.0110, 577.0082 Found: m/z 573.0141, 575.0036, 576.9989 $([M + H])^+$.

4.1.17. 3-[5-Bromo-1-(4-chlorobenzoyl)-1H-indol-3-ylmethylene]-1-(2,6-dichlorophenyl)-1,3-dihydroindol-2-one, ***16***

Pure product was obtained as a yellow solid in a yield of 70%, mp 240 °C (decomposed); IR ν_{max} (KBr, cm^{-1}): 1677 (C=O); ^1H NMR (300 MHz, DMSO-d_6) δ ppm: 6.43 (d, J = 6.6 Hz, 1H, ArH), 7.15 (s, 2H, ArH), 7.32 (d, J = 8.1 Hz, 2H, ArH), 7.41 (d, J = 8.4 Hz, 2H, ArH), 7.53 (d, J = 7.5 Hz, 1H, ArH), 7.62 (d, J = 7.8 Hz, 3H, ArH), 7.91–7.96 (m, 2H, ArH), 8.21 (s, 1H, bridged =CH), 8.29 (s, 1H, ArH), 9.43 (s, 1H, indole 2-H); ^{13}C NMR ($CDCl_3$ + DMSO-d_6) δ ppm: 107.85, 110.40, 113.28, 113.77, 116.89, 117.67, 119.82, 121.52, 124.42, 124.63, 126.22, 127.35, 128.23, 129.30, 129.45, 129.99, 130.08, 130.30, 134.27, 134.74, 134.92, 134.98, 138.03, 140.27, 164.98 (C=O), 167.00 (C=O); HRMS (ESI) Calcd for $C_{30}H_{16}BrCl_3O_2N_2$: 620.9533, 622.9513, 624.9485. Found m/z 617.0165, 619.0143, 621.0115.

4.1.18. 3-[5-Bromo-1-(2-fluorobenzyl)-1H-indol-3-ylmethylene]-1-(2,6-dichlorophenyl)-1,3-dihydroindol-2-one, ***17***

Pure product was obtained as a yellow solid in a yield of 82%, mp 280 °C (decomposed); IR ν_{max} (KBr, cm^{-1}): 1703 (C=O); ^1H NMR (300 MHz, $CDCl_3$) δ ppm: 5.42 (s, 2H, CH_2), 6.45–6.48 (dd, J = 2.4 Hz, J = 6.6 Hz, 1H, ArH), 6.90 (t, J = 7.2 Hz, 1H, ArH), 7.00 (t, J = 7.5 Hz, 1H, ArH), 7.04–7.10 (m, 1H, ArH), 7.15–7.25 (m, 4H, ArH), 7.34–7.41 (m, 2H, ArH), 7.54 (d, J = 8.1 Hz, 2H, ArH), 7.74–7.76 (dd, J = 1.8 Hz, J = 5.4 Hz, 1H, ArH), 7.97 (s, 1H, ArH), 8.08 (s, 1H, bridged =CH), 9.58 (s, 1H, indole 2-H); HRMS (ESI) Calcd for $C_{30}H_{18}BrCl_2FON_2$: 612.9856, 614.9835, 616.9807 Found: m/z 612.9858, 614.9840, 616.9815 $([M + Na])^+$.

4.1.19. 5-[5-Bromo-1-(2-fluorobenzyl)-1H-indol-3-ylmethylene] pyrimidine-2,4,6-trione, ***18***

Pure product was obtained as a yellow solid in a yield of 80%, mp >300 °C; IR ν_{max} (KBr, cm^{-1}): 1654, 1685, 1724 (C=O), 3189, 3431 (NH); ^1H NMR (300 MHz, DMSO-d_6) δ ppm: 5.67 (s, 2H, CH_2), 7.14–7.23 (m, 2H, ArH), 7.29–7.39 (m, 2H, ArH), 7.45 (d, J = 8.4 Hz, 1H, ArH), 7.65 (d, J = 8.7 Hz, 1H, ArH), 8.02 (s, 1H, bridged =CH), 8.60 (s, 1H, ArH), 9.60 (s, 1H, indole 2-H), 11.10 (s, 1H, NH), 11,18 (s, 1H, NH); HRMS (ESI) Calcd for $C_{20}H_{13}BrFO_3N_3$: 442.0197, 444.0178. Found: m/z 442.0379, 444.0354 $([M + H])^+$.

4.1.20. 3-(1-Benzyl-5-bromo-1H-indol-3-ylmethylene)-1,3-dihydroindol-2-one, ***19***

Pure product was obtained as a yellow solid in a yield of 77%, mp 280–281 °C; IR ν_{max} (KBr, cm^{-1}): 1678 (C=O), 3200 (NH); ^1H NMR (300 MHz, DMSO-d_6) δ ppm: 5.56 (s, 2H, CH_2), 6.84 (d, J = 7.5 Hz, 1H, ArH), 6.97 (t, J = 7.5 Hz, 1H, ArH), 7.13 (t, J = 7.2 Hz, 1H, ArH), 7.23–7.34 (m, 6H, ArH), 7.49 (d, J = 8.4 Hz, 1H, ArH), 7.92 (d, J = 7.2 Hz, 1H, ArH), 8.09 (s, 1H, bridged =CH), 8.46 (s, 1H, ArH) 9.55 (s, 1H, indole 2-H), 10.48 (s, 1H, NH); ^{13}C NMR (DEPT-135) ($CDCl_3$ + DMSO-d_6) δ ppm: 50.06 (−ve, CH_2), 108.86 (+ve, CH), 110.55 (+ve, CH), 112.65 (+ve, CH), 114.16 (C), 118.98 (+ve, CH), 120.35 (+ve, CH), 121.33 (C), 125.04 (C), 125.36 (+ve, CH), 125.64 (+ve, CH), 126.86 (+ve, CH), 127.55 (+ve, CH), 128.53 (+ve, CH), 130.63 (C), 134.51 (C), 136.57 (C), 136.94 (+ve, CH), 139.32 (C), 167.94 (C=O); HRMS (ESI) Calcd for $C_{24}H_{17}BrON_2$: 429.0597, 431.0578. Found: m/z 429.0659, 431.0641 $([M + H])^+$.

4.1.21. 3-[5-Bromo-1-(4-chlorobenzoyl)-1H-indol-3-ylmethylene]-1,3-dihydroindol-2-one, ***20***

Pure product was obtained as a yellow solid in a yield of 65%, mp 280 °C (decomposed); IR ν_{max} (KBr, cm^{-1}): 1683 (C=O), 3254 (NH); ^{1}H NMR (300 MHz, DMSO-d_6) δ ppm: 6.87 (t, J = 7.2 Hz, 1H, ArH), 6.98 (t, J = 7.8 Hz, 1H, ArH), 7.12 (t, J = 7.5 Hz, 1H, ArH), 7.30 (s, 1H, ArH), 7.39 (d, J = 8.4 Hz, 1H, ArH), 7.67–7.89 (m, 4H, ArH), 8.01 (s, 1H, bridged =CH), 8.10 (s, 1H, ArH), 9.47 (s, 1H, indole 2-H), 10.15 (s, 1H, ArH), 11.77 (s, 1H, NH); HRMS (ESI) Calcd for $C_{24}H_{14}BrClO_2N_2$: 498.9819, 500.9799 Found: m/z 498.9612, 500.9597 $([M + Na])^+$.

4.1.22. 3-[5-Bromo-1-(2,6-dichlorobenzoyl)-1H-indol-3-ylmethylene]-1,3-dihydroindol-2-one, ***21***

Pure product was obtained as a yellow solid in a yield of 86%, mp 270 °C (decomposed); IR ν_{max} (KBr, cm^{-1}): 1709 (C=O), 3190 (NH); ^{1}H NMR (400 MHz, DMSO-d_6) δ ppm: 6.76 (t, J = 7.6 Hz, 1H, ArH), 6.84 (t, J = 8.0 Hz, 1H, ArH), 7.16–7.22 (m, 1H, ArH), 7.39 (d, J = 7.6 Hz, 1H, ArH), 7.58 (s, 1H, ArH), 7.64–7.78 (m, 4H, ArH), 7.93–8.05 (m, 1H, ArH), 8.47–8.52 (m, 1H, ArH), 9.25 (s, 1H, indole 2-H), 10.55 (s, 1H, NH); HRMS (ESI) Calcd for $C_{24}H_{13}BrCl_2O_2N_2$: 510.9610, 512.9589, 514.9561 Found: m/z 510.9830, 512.9607, 514.9832 $([M + H])^+$.

4.1.23. 4-(1-Benzyl-5-methoxy-1H-indol-3-ylmethylene)-2-(3-chlorophenyl)-5-methyl-2,4-dihydropyrazol-3-one, ***22***

Pure product was obtained as a yellow solid in a yield of 70%, mp 181–183 °C; IR ν_{max} (KBr, cm^{-1}): 1676 (C=O); ^{1}H NMR (300 MHz, $CDCl_3$) δ ppm: 2.35 (s, 3H, CH_3), 3.91 (s, 3H, OCH_3), 5.43 (s, 2H, CH_2), 7.17–7.21 (m, 4H, ArH), 7.25 (s, 1H, ArH), 7.29–7.37 (m, 4H, ArH), 7.75 (s, 1H, ArH), 7.87 (d, J = 8.1 Hz, 1H, ArH), 7.99 (s, 1H, bridged =CH), 8.10 (s, 1H, ArH), 9.93 (s, 1H, indole 2-H); ^{13}C NMR (DEPT-135) ($CDCl_3$) δ ppm: 13.15 (+ve, CH_3), 51.85 (−ve, CH_2), 55.75 (+ve, CH_3), 110.84 (C), 112.90 (+ve, CH), 116.45 (C), 116.66 (+ve, CH), 118.82 (+ve, CH), 120.90 (+ve, CH), 121.03 (C), 124.29 (+ve, CH), 126.66 (+ve, CH), 127.48 (C), 128.33 (+ve, CH), 129.09 (+ve, CH), 134.49 (C), 134.68 (+ve, CH), 134.94 (C), 136.14 (+ve, CH), 139.75 (C), 141.48 (C), 150.33 (C), 162.91 (C=O); HRMS (ESI) Calcd for $C_{27}H_{22}ClO_2N_3$: 478.1293, 480.1266. Found: m/z 478.1300, 480.1280 $([M + Na])^+$.

4.1.24. 3-(1-Benzyl-5-methoxy-1H-indol-3-ylmethylene)-1-(2,6-dichlorophenyl)-1,3-dihydro-indol-2-one, ***23***

Pure product was obtained as a yellow solid in a yield of 60%, mp 153–155 °C; ν_{max} (KBr, cm^{-1}): 1688 (C=O); ^{1}H NMR (300 MHz, $CDCl_3$) δ ppm: 3.94 (s, 3H, OCH_3), 5.36 (s, 2H, CH_2), 6.46–6.49 (m, 1H, ArH), 6.85–6.89 (dd, J = 2.1 Hz, J = 8.7 Hz, 1H, ArH), 7.14–7.18 (m, 6H, ArH), 7.23–7.30 (m, 2H, ArH), 7.38–7.40 (m, 2H, ArH), 7.52 (s, 1H, ArH), 7.55 (s, 1H, ArH), 7.75–7.78 (m, 1H, ArH), 8.06 (s, 1H, bridged =CH), 9.58 (s, 1H, indole 2-H); ^{13}C NMR ($CDCl_3$) δ ppm: 50.99 (CH_2), 55.50 (CH_3), 100.20, 108.22, 110.79, 111.33, 112.10, 116.62, 117.60, 121.70, 125.01, 126.21, 126.26, 127.40, 127.55, 128.37, 128.47, 129.99, 130.80, 130.87, 135.53, 135.69, 137.84, 138.36, 155.35, 165.63 (C=O); HRMS (ESI) Calcd for $C_{31}H_{22}Cl_2O_2N_2$: 547.0951, 549.0923 Found: m/z 547.1022, 549.0966 $([M + Na])^+$.

4.1.25. 5-(1-Benzyl-5-methoxy-1H-indol-3-ylmethylene) pyrimidine-2,4,6-trione, ***24***

Pure product was obtained as a yellow solid in a yield of 82%, mp >300 °C; IR ν_{max} (KBr, cm^{-1}): 1649, 1678, 1719 (C=O), 3167, 3199 (NH); ^{1}H NMR (300 MHz, DMSO-d_6) δ ppm: 3.85 (s, 3H, OCH_3), 5.61 (s, 2H, CH_2), 6.92 (dd, J = 2.4 Hz, J = 9.0 Hz, 1H, ArH), 7.28–7.37 (m, 6H, ArH), 7.55 (d, J = 8.7 Hz, 1H, ArH), 8.62 (s, 1H, bridged =CH), 9.53 (s, 1H, indole 2-H), 10.99 (s, 1H, NH), 11.05 (s, 1H, NH); ^{13}C NMR (DMSO-d_6) δ ppm: 50.53 (CH_2), 55.57 (CH_3), 100.29, 108.21, 110.85, 113.04, 113.35, 127.52, 127.99, 128.82, 131.03, 136.10, 142.05, 143.08, 150.36, 156.48 (C=O), 163.18 (C=O), 164.50 (C=O); HRMS (ESI) Calcd for $C_{21}H_{17}O_4N_3$: 398.1111. Found: m/z 398.1128 $([M + Na])^+$.

4.1.26. 3-(1-Benzyl-5-methoxy-1H-indol-3-ylmethylene)-1,3-dihydroindol-2-one, ***25***

Pure product was obtained as a yellow solid in a yield of 67%, mp 246 °C; IR ν_{max} (KBr, cm^{-1}): 1680 (C=O), 3200 (NH); ^{1}H NMR (300 MHz, $CDCl_3$) δ ppm: 3.91 (s, 3H, OCH_3), 5.38 (s, 2H, CH_2), 6.85 (d, J = 7.5 Hz, 2H, ArH), 7.05 (t, J = 7.5 Hz, 1H, ArH), 7.13–7.33 (m, 8H, ArH), 7.62 (d, J = 7.2 Hz, 1H, ArH), 7.70 (s, 1H, ArH), 7.90 (s, 1H, bridged =CH), 9.49 (s, 1H, indole 2-H); ^{13}C NMR (DEPT-135) ($CDCl_3$ + DMSO-d_6) δ ppm: 50.61 (−ve, CH_2), 55.37 (+ve, CH_3), 100.08 (+ve, CH), 108.82 (+ve, CH), 110.54 (C), 111.03 (+ve, CH), 111.96 (+ve, CH), 117.40 (+ve, CH), 118.76 (C), 120.27 (+ve, CH), 125.42 (C), 125.64 (+ve, CH), 126.19 (+ve, CH), 126.28 (+ve, CH), 127.29 (+ve, CH), 128.26 (+ve, CH), 129.63 (C), 130.70 (C), 135.82 (C), 136.76 (+ve, CH), 138.59 (C), 155.08 (C), 168.34 (C=O); HRMS (ESI) Calcd for $C_{25}H_{20}O_2N_2$: 403.1417. Found: m/z 403.1439 $([M + Na])^+$.

4.1.27. 1-(2,6-Dichlorophenyl)-3-(2-trifluoromethylbenzylidene)-1,3-dihydroindol-2-one, ***27***

Pure product was obtained as a light yellow solid in a yield of 84%, mp 134–135 °C; IR ν_{max} (KBr, cm^{-1}): 1658 (C=O); ^{1}H NMR (300 MHz, $CDCl_3$) δ ppm: 6.41 (d, J = 7.8 Hz, 1H, ArH), 6.85 (t, J = 7.5 Hz, 1H, ArH), 7.07 (d, J = 7.8 Hz, 1H, ArH), 7.18 (t, J = 7.8 Hz, 1H, ArH), 7.37–7.42 (m, 1H, ArH), 7.52–7.67 (m, 4H, ArH), 7.82 (t, J = 7.8 Hz, 2H, ArH), 8.09 (s, 1H, bridged =CH); HRMS (ESI) Calcd for $C_{22}H_{12}Cl_2F_3ON$: 456.0140, 458.0112. Found: m/z 456.0136, 458.0108 $([M + Na])^+$.

4.1.28. 2-(3-Chlorophenyl)-5-methyl-4-(2-trifluoromethylbenzylidene)-2,4-dihydropyrazol-3-one, ***28***

Pure product was obtained as an orange solid in a yield of 81%, mp 103–104 °C; IR ν_{max} (KBr, cm^{-1}): 1701 (C=O); ^{1}H NMR (300 MHz, $CDCl_3$) δ ppm: 2.36 (s, 3H, CH_3), 7.14 (d, J = 7.5 Hz, 1H, ArH), 7.32 (d, J = 7.8 Hz, 1H, ArH), 7.61–7.70 (m, 2H, ArH), 7.77–7.86 (m, 3H, ArH), 8.00 (s, 1H, bridged =CH), 8.43 (d, J = 7.8 Hz, 1H, ArH); ^{13}C NMR (DEPT-135) ($CDCl_3$) δ ppm: 13.53 (+ve, CH_3), 107.64 (C), 116.89 (+ve, CH), 119.04 (+ve, CH), 125.31 (+ve, CH), 126.52 (+ve, CH), 129.94 (+ve, CH), 130.29 (C), 131.87 (+ve, CH), 131.95 (C), 132.99 (+ve, CH), 135.02 (C), 139.49 (C), 142.37 (+ve, CH), 151.30 (C), 161.51 (C=O); HRMS (ESI) Calcd for $C_{18}H_{12}ClF_3ON_2$: 387.0482 Found: m/z 387.0491 $([M + Na])^+$.

4.1.29. 1-(4-Chlorobenzoyl)-3-(2-trifluoromethylbenzylidene)-1,3-dihydroindol-2-one, ***29***

Pure product was obtained as a light yellow solid in a yield of 61%, mp 199–200 °C; IR ν_{max} (KBr, cm^{-1}): 1682, 1722 (C=O); ^{1}H NMR (300 MHz, $CDCl_3$) δ ppm: 6.98 (t, J = 7.5 Hz, 1H, ArH), 7.09 (d, J = 7.8 Hz, 1H, ArH), 7.36 (t, J = 7.8 Hz, 1H, ArH), 7.49 (d, J = 8.1 Hz, 2H, ArH), 7.57–7.76 (m, 5H, ArH), 7.83 (d, J = 7.5 Hz, 1H, ArH), 7.91 (d, J = 8.1 Hz, 1H, ArH), 7.96 (s, 1H, bridged =CH); ^{13}C NMR (DEPT-135) ($CDCl_3$) δ ppm: 106.53 (C), 115.54 (+ve, CH), 121.60 (C), 122.90 (+ve, CH), 124.57 (+ve, CH), 126.60 (+ve, CH), 128.12 (C), 128.54 (+ve, CH), 129.60 (C), 129.68 (+ve, CH), 130.67 (+ve, CH), 130.86 (+ve, CH), 132.02 (+ve, CH), 132.68 (C), 133.10 (C), 134.88 (+ve, CH), 139.24 (C), 140.58 (C), 166.74 (C=O), 168.22 (C=O); HRMS (ESI) Calcd for $C_{23}H_{13}ClF_3O_2N$: 450.0479, 452.0451. Found: m/z 450.0913, 452.0892 $([M + Na])^+$.

4.1.30. 1-(2-Fluorobenzyl)-3-(2-trifluoromethylbenzylidene)-1,3-dihydroindol-2-one, ***30***

Pure product was obtained as a yellow solid in a yield of 73%, mp 135–136 °C; IR ν_{max} (KBr, cm^{-1}): 1649 (C=O); ^{1}H NMR (300 MHz,

$CDCl_3$) δ ppm: 5.05 (s, 2H, CH_2), 6.79 (t, $J = 8.1$ Hz, 2H, ArH), 6.96 (d, $J = 7.2$ Hz, 1H, ArH), 7.06–7.19 (m, 3H, ArH), 7.23 (s, 1H, ArH), 7.34 (t, $J = 7.2$ Hz, 1H, ArH), 7.53–7.64 (m, 2H, ArH), 7.70 (d, $J = 6.9$ Hz, 1H, ArH), 7.81 (d, $J = 7.5$ Hz, 1H, ArH), 8.04 (s, 1H, bridged =CH); HRMS (ESI) Calcd for $C_{23}H_{15}F_3ON$: 420.0982. Found: m/z 420.1032 $([M + Na])^+$.

4.2. Procedure for in vitro anticancer screening

Anticancer screening of compounds was carried out at National Cancer Institute, Bethesda, MD, USA as per the standard procedure [20]. Human tumor cell lines of the cancer screening panel were grown in RPMI 1640 medium containing 5% fetal bovine serum and 2 mM L-glutamine. Cells were inoculated into 96 well microtiter plates in 100 μL at plating densities ranging from 5000 to 40,000 cells/well depending on the doubling time of individual cell lines. After cell inoculation, the microtiter plates were incubated at 37 °C, 5% CO_2, 95% air and 100% relative humidity for 24 h prior to addition of experimental drugs. After 24 h, two plates of each cell line were fixed *in situ* with TCA, to represent a measurement of the cell population for each cell line at the time of compound addition (Tz). Compounds were solubilized in dimethyl sulfoxide at 400-fold the desired final maximum test concentration and stored frozen prior to use. At the time of compound addition, an aliquot of frozen concentrate was thawed and diluted to twice the desired final maximum test concentration with complete medium containing 50 μg/ml gentamicin. Additional four, 10-fold or ½ log serial dilutions were made to provide a total of five compound concentrations plus control. Aliquots of 100 μL of these different drug dilutions were added to the appropriate microtiter well already containing 100 μL of medium, resulting in the required final concentrations. Following compound addition, the plates were incubated for an additional 48 h at 37 °C, 5% CO_2, 95% air, and 100% relative humidity. For adherent cells, the assay was terminated by the addition of cold TCA. Cells were fixed *in situ* by the gentle addition of 50 μL of cold 50% (w/v) TCA (final concentration, 10% TCA) and incubated for 60 min at 4 °C. The supernatant was discarded, and the plates were washed five times with tap water and air dried. Sulforhodamine B (SRB) solution (100 μL) at 0.4% (w/v) in 1% acetic acid was added to each well, and plates were incubated for 10 min at room temperature. After staining, unbound dye was removed by washing five times with 1% acetic acid and the plates were air dried. Bound stain was subsequently solubilized with 10 mM trizma base, and the absorbance was read on an automated plate reader at a wavelength of 515 nm. Using the absorbance measurements [time zero, (Tz), control growth, (C), and test growth in the presence of compound at five concentration levels (Ti)], the percentage growth was calculated at each of the compound concentrations. Percentage growth inhibition was calculated as

$$[(\mathrm{Ti} - \mathrm{Tz})/(\mathrm{C} - \mathrm{Tz})] \times 100 \text{ for conc for which } \mathrm{Ti} \geq \mathrm{Tz}$$

$$[(\mathrm{Ti} - \mathrm{Tz})/\mathrm{Tz}] \times 100 \text{ for conc for which } \mathrm{Ti} < \mathrm{Tz}$$

Growth inhibition of 50% (GI_{50}) was calculated from $[(Ti - Tz)/(C - Tz)] \times 100 = 50$, which was the compound concentration resulting in a 50% reduction in the net protein increase (as measured by SRB staining) in control cells during the drug incubation. The LC_{50} (concentration of drug resulting in a 50% reduction in the measured protein at the end of the drug treatment as compared to that at the beginning) indicating a net loss of cells following treatment was calculated from $[(Ti - Tz)/Tz] \times 100 = -50$. Values were calculated for each of these two parameters if the level of activity was reached; however, if the effect was not reached or exceeded, the value for that parameter was expressed as greater or less than the maximum or minimum concentration tested.

4.3. UV–vis spectral studies

UV–visible spectral studies were performed on Biotek powerwaveXS spectrophotometer. The stock solution for both the compounds and the enzyme were prepared in HPLC grade DMSO. The conc of the compound stock solution was kept at 10^{-3} M and was diluted accordingly to get the final conc of 1 μM–5 μM. 50 μL of the enzyme was diluted to 1000 μL (2.89 μM) for further titration with compound solution.

4.4. Procedure for dihydrofolate reductase inhibition assay

The dihydrofolate reductase inhibition assay was performed as per the manual of DHFR assay kit (SIGMA Product Code CS0340). All the dilutions were made in assay buffer pH 7.5. 10 mM stock solutions of dihydrofolic acid and NADPH in assay buffer were prepared. Stock solutions of the test compounds with different conc were prepared in DMSO and 20 μL of each were taken to attain final conc of 10^{-8} M, 10^{-7} M, 10^{-6} M and 10^{-5} M in the respective wells of 96 well plate containing assay buffer. 0.1 units of DHFR as supplied in the kit were diluted and 20 μL of its 3×10^{-3} units were used in each reaction. Each well of the 96 well plate was charged with 157.8 μL assay buffer. 1.2 μL of NADPH solution was added to each well except 1A, 1B (blank well). 20 μL of test compound (including methotrexate as positive control) was added to each well except 1A–1H. Reaction was started by the addition of 1 μL of dihydrofolic acid to each well except 1C and 1D. 1G and 1H contained 20 μL of DMSO to check any inhibition of enzyme activity due to DMSO. The change in absorbance at 340 nm was monitored as a function of time. Percentage inhibition of enzymatic activity was calculated after nullifying the effects of NADPH, folate and solvent. IC_{50} was calculated by plotting a graph between percentage inhibitions and corresponding conc of the compound using Graphpad Prism version 6.01.

4.5. Molecular docking

Compounds were built using the builder tool kit of the software package Argus Lab 4.0.1 [21] and energy minimized with semi-empirical quantum mechanical method PM3. Crystal co-ordinates of DHFR (PDB ID 3GHW) was downloaded from protein data bank and in the molecule tree view of the software, the monomeric structures of the crystal coordinate was selected and the active site was defined as 15 Å around the ligand.

The molecule to be docked in the active site of the enzyme was pasted in the work space carrying the structure of the enzyme. The docking programme implements an efficient grid based docking algorithm which approximates an exhaustive search within the free volume of the binding site cavity. The conformational space was explored by the geometry optimization of the flexible ligand (rings were treated as rigid) in combination with the incremental construction of the ligand torsions. Thus, docking occurs between the flexible ligand parts of the compound and enzyme. Docking was repeated several times (approx. 10000 iterations) until no change in position of the ligand and a constant value of binding energy was observed. The ligand orientation was determined by a shape scoring function based on Ascore and final positions were ranked by lowest interaction energy values. H-bonds and hydrophobic interactions between the respective compound and enzyme were explored.

Acknowledgments

Financial assistance from CSIR, New Delhi and DST, New Delhi is gratefully acknowledged. Shaveta thanks UGC for fellowship. National Cancer Institute, Bethesda USA is acknowledged for anticancer screening of compounds. Authors gratefully acknowledge the contributions of Prof. A.S. Brar, vice-chancellor, GNDU for creating state of the art research facilities.

Appendix A. Supplementary data

Supplementary data related to this article can be found at http://dx.doi.org/10.1016/j.ejmech.2013.12.047.

References

[1] World Health Organization, Fact sheet No. 297, February, 2012.
[2] S.P. Gupta, Chem. Rev. 94 (1994) 1507–1551.
[3] U. Galm, M.H. Hager, S.G.J. Van Lanen Ju, J.S. Thorson, B. Shen, Chem. Rev. 105 (2005) 739–758.
[4] D.E. Thurston, Chemistry and Pharmacology of Anticancer Drugs, CRC Press, Taylor & Francis Group, New York, 2007.
[5] J.J. Guidry, A. Greisinger, L.A. Aday, R.J. Winn, S. Vernon, T.A. Throckmorton, Oncol. Nurs. Forum 23 (1996) 1393–1398.
[6] I.F. Tannock, C.M. Lee, J.K. Tunggal, D.S.M. Cowan, M.J. Egorin, Clin. Cancer Res. 8 (2002) 878–884.
[7] J.A. Ajani, R.J. Mayer, D.M. Ota, G.D. Steele, D. Evans, M. Roh, D.J. Sugarbaker, P. Dumas, C. Gray, D.A. Vena, D.M. Stablein, J. Natl. Cancer Inst. 85 (1993) 1839–1844.
[8] P.A. Bunn Jr., K. Kelly, Clin. Cancer Res. 4 (1998) 1087–1100.
[9] P. Singh, A. Bhardwaj, Mini Rev. Med. Chem. 8 (2008) 388–398 (and references therein).
[10] W.B. Parker, Chem. Rev. 109 (2009) 2880–2893.
[11] J.L. Grem, Invest. New Drugs 18 (2000) 299–313.
[12] F.M. Huennekens, Adv. Enzyme Regul. 34 (1994) 397–419.
[13] S. Chattopadhyay, R.G. Moran, I.D. Goldman, Mol. Cancer Ther. 6 (2007) 404–417.
[14] P. Singh, M. Kaur, P. Verma, Bioorg. Med. Chem. Lett. 19 (2009) 3054–3058.
[15] P. Singh, M. Kaur, W. Holzer, Eur. J. Med. Chem. 45 (2010) 4968–4982.
[16] P. Singh, M. Kaur, Shaveta, J. Med. Chem. 55 (2012) 6381–6390.
[17] P. Singh, A. Bhardwaj, J. Med. Chem. 53 (2010) 3707–3717.
[18] Dihydrofolate Reductase Inhibition Assay Kit. SIGMA Product Code CS0340.
[19] A. Gangjee, W. Li, R.L. Kisliuk, V. Cody, J. Race, J. Piriano, J. Makin, J. Med. Chem. 52 (2009) 4892–4902.
[20] www.dtp.nci.nih.gov.
[21] ArgusLab 4.0.1, M. A. Thompson, Planaria Software LLC, Seattle, WA 98155.